British Journal of Pharmacology (1999) 126, 1691–1698 
http://www.stockton-press.co.uk/bjp

# Modification of membrane currents in mouse neuroblastoma cells following infection with rabies virus

[1]M. Iwata, [1]S. Komori, [1]T. Unno, [2]N. Minamoto & *,[1]H. Ohashi

[1]Laboratory of Pharmacology, Department of Veterinary Science, Faculty of Agriculture, Gifu University, Gifu 501-1112 Japan and [2]Laboratory of Veterinary Public Health, Department of Veterinary Science, Faculty of Agriculture, Gifu University, Gifu 501-1112, Japan

**1** The effect on membrane currents of infection of mouse neuroblastoma NA cells with rabies virus was studied by using the whole-cell patch clamp technique.

**2** Three types of membrane currents, namely voltage-dependent $Na^+$ current ($I_{Na}$), delayed rectifier $K^+$ current ($I_{K\text{-}DR}$) and inward rectifier $K^+$ current ($I_{K\text{-}IR}$) were elicited in uninfected cells.

**3** In cells 3 days after infection with the virus, no detectable change was observed in morphology and membrane capacitance, but $I_{Na}$ and $I_{K\text{-}IR}$ were significantly decreased in amplitude without any appreciable difference in the time course of current activation and inactivation. The voltage-dependence of $I_{Na}$ activation was significantly shifted in the positive direction along the voltage axis with a decreased slope. $I_{K\text{-}DR}$ remained almost unaltered after the viral infection.

**4** The resting membrane potential, measured with a physiological $K^+$ gradient across the cell membrane, was decreased (depolarized) after the viral infection. The depolarization was associated with the decreased amplitude of $I_{K\text{-}IR}$.

**5** These results suggest that infection of mouse neuroblastoma NA cells with rabies virus causes reduction of functional expression of ion channels responsible for $I_{Na}$ and $I_{K\text{-}IR}$, and provide evidence for possible involvement of the change in membrane properties in the pathogenesis of rabies disease.

**Keywords:** Rabies virus; viral infection; neuroblastoma; $Na^+$ current; $K^+$ current; membrane potential; whole-cell patch clamp

**Abbreviations:** ACh, acetylcholine; $E_m$, membrane potential; $G_{Na}$, $Na^+$ conductance; $G_{Na\text{-}max}$, maximal $G_{Na}$; HEPES, 2-[4-(2-hydroxyethl)-1-piperazinyl]ethanesulphonic acid; IgG, immunoglobulin G; $I_{K\text{-}DR}$, delayed rectifier $K^+$ current; $I_{K\text{-}IR}$, inward rectifier $K^+$ current; $I_{Na}$, voltage-dependent $Na^+$ current; N protein, nucleoprotein; NA cells, subcloned cells from Neuro-2a, a clonal line of C-1300 mouse neuroblastoma; p.f.u., plaque forming units; TEA, tetraethylammonium chloride; TTX, tetrodotoxin; $V_{0.5}$, voltage when $G_{Na}$ reached to half of the maximal $G_{Na}$; $\kappa$, slope factor

## Introduction

Rabies disease in several natural hosts, including human beings is characterized by symptoms of aggression, restlessness, fluctuating consciousness between hyperexcitation and relapse, and generalized convulsion. Immunohistochemical study of human rabies cases revealed that brainstem and spinal cord are predilection sites for rabies virus infection (Tirawatnpong *et al*., 1989). This was also true in mice and other some species (Johnson, 1965; Jackson & Reimer, 1989; Smart & Charlton, 1992; Sugamata *et al*., 1992). Interestingly, there have been found little or no histopathological changes in the central nervous system in spite of the characteristic symptoms. Under these circumstances, it is believed that the pathogenesis of this disease may be due to their functional impairment of host neurons.

It has been suggested that rabies virus infection affects the function of $\gamma$-amino-n-butryic acid (Ladogana *et al*., 1994), acetylcholine (ACh, Tsiang, 1982; Dumrongphol *et al*., 1996), serotonin (Ceccaldi *et al*., 1993) and opioid (Munzel & Koschel, 1981) systems in the brain. However, there is no paper dealing with a question whether rabies virus infection modifies membrane ion channels of neurons which determine the initial, essential responses to neurotransmitters.

Recently, Bakhramov *et al*. (1995) have demonstrated in human fibroblast cells that cytomegalovirus infection alters the expression profile of voltage-dependent $Na^+$ channel and delayed rectifier $K^+$ channel which are involved in discharge of an action potential of excitable cells.

In the present study, we measured membrane currents using the whole-cell patch clamp technique to study effects of rabies virus infection on ion channels in subcloned cells (NA cells) from Neuro-2a, a clonal line of C-1300 mouse neuroblastoma (McMorris & Ruddle, 1974). This cell type has been shown to be sensitive to rabies virus (Iwasaki & Clark, 1977). The results suggest that in NA cells, rabies virus infection reduces functional expression of both voltage-dependent $Na^+$ channel and inward rectifier $K^+$ channel without changing that of delayed rectifier $K^+$ channel.

## Methods

### *Cell culture*

Mouse neuroblastoma NA cells were obtained as a monolayer culture with 30–50 passages from Laboratory of Veterinary Public Health, Gifu University. The cells were cultured for 5 days in Eagle's minimum essential medium with foetal calf serum (10%), penicillin (10 units $ml^{-1}$), streptomycin

*Author for correspondence.

(0.01 g $ml^{-1}$), fungizone (2.5 $\mu$g $ml^{-1}$) and $NaHCO_3$ (0.1–0.15%) and then for 2 days in another medium, maintenance medium having the same composition as above but a reduced foetal calf serum (5%). After the 7 day culture, cells confluent in glass culture flasks were trypsinized, and then suspended in trypsin-free maintenance medium. Dimethylsulphoxide (1–2%) was added to this medium to facilitate differentiation (Baumgold & Spector, 1987; Clejan *et al*., 1996) and to prevent their excessive growth of the cells. Cell suspension was seeded into a 24 well plate containing glass coverslips (14 mm in diameter) in aliquots which contained each $1-1.5\times10^4$ cells, and placed in a humidified atmosphere of 5% $CO_2$ at 37°C for 5–8 days before virus inoculation.

### *Virus infection*

Rabies virus (RC-HL strain, Ito *et al*., 1994) was propagated in baby hamster kidney cells cultured in Eagle's minimum essential medium with calf serum (5%), tryptose phosphate broth (5%), penicillin (10 units $ml^{-1}$), streptomycin (0.01 g $ml^{-1}$), fungizone (2.5$\mu$g $ml^{-1}$) and $NaHCO_3$ (0.1–0.15%) at 37°C for 3–4 days. The culture medium was collected and centrifuged at 3500 r.p.m. for 5 min. The supernatant was divided into small fractions and stored at −80°C until use. The titer of the stock virus solutions was $4.5-5.7\times10^7$ plaque forming units (p.f.u.) $ml^{-1}$.

The coverslips of NA cells prepared in the 24 well plate were divided into two groups, one of which was then inoculated with rabies virus at a multiplicity of infection of 50 p.f.u. per cell, and the other was mock inoculated as a control. After incubation with or without the virus inoculum for 1 h at 37°C, the cells were cultured for 3 days under the same conditions as before virus inoculation (see above).

An indirect immunofluorescence technique was used to detect intracytoplasmic rabies virus nucleoprotein (N protein), as previously described (Minamoto *et al*., 1994). Briefly, NA cells, which were cultured for 3 days after virus inoculation or mock inoculation, were air-dried, fixed with cold acetone (−20°C) for 15 min, and then subjected to a sequential immuno staining with a mouse monoclonal anti-N protein (Laboratory of Veterinary Public Health, Gifu University) followed by a fluorescein isothiocyanate-conjugated anti-mouse immunoglobulin G (IgG) rabbit antibody (ICN Immuno Biologicals; California, U.S.A.).

All virus-inoculated cells expressed the viral N protein immunoreactivity, indicating their infection with the virus. On the other hand, no such immunoreactivity was seen in mock-inoculated cells. The two types of cells prepared were used as virus-infected and uninfected cells for the following experiments.

### *Current and potential recordings*

A coverslip with virus-infected or uninfected NA cells was placed in a 0.5 ml organ bath on the stage of an inverted microscope (TMD, Nikon, Chiyoda-ku, Tokyo), and the organ bath was perfused with a physiological salt solution (PSS; the composition given below) at a rate of 5–10 ml $min^{-1}$ for 1–2 min to wash away the culture medium and debris. The cells were then equilibrated with the PSS for 3–5 min before starting experiments.

Recordings of whole-cell membrane currents and changes in membrane potential were made at room temperature (23–27°C), using standard patch clamp techniques (Hamill *et al*., 1981). Patch pipettes had a resistance of 4–6 MΩ when filled with a pipette solution. Command pulses of voltage or current were generated by an electrical stimulator (SET-1201, Nihon Kohden, Shinjuku-ku, Tokyo). The resulting signals were amplified by a patch-clamp amplifier (CEZ-2300, Nihon Kohden, Shinjuku-ku, Tokyo) and stored on a pulse code modulation data recorder (RD-111T, TEAC, Musashino City, Tokyo) for analysis and illustration. Data analysis was performed on a computer (Apple Macintosh Performa 5320), using a data acquisition and analysis instrument (MacLab4, ADInstruments, Castle Hill, NSW, Australia). The current signals were filtered at a cut-off frequency of 1 kHz and digitized with a sampling rate of 1–40 kHz.

Membrane currents activated by voltage pulses were measured without making any capacitance compensation, because the prepared circuitry for the compensation was not effective enough especially when pulses of 50 mV or larger were used for activation. Therefore, a capacitative transient and a rapidly-activated $Na^+$ current ($I_{Na}$) would overlap each other. To confirm this, a current (referred to as crude $I_{Na}$) was elicited by a 50 ms step pulse from −80 to −10 mV, and then this was repeated after application of TTX (1 $\mu$M). A TTX-sensitive current, $I_{Na}$, was obtained by subtracting a current elicited by the second pulse from the crude $I_{Na}$. The crude $I_{Na}$ was found to be smaller in amplitude by $11.3\pm1.2\%$, longer in time-to-peak by $4.1\pm0.7\%$, and shorter in half-decay time by $3.7\pm1.7\%$, in uninfected cells ($n=5$). The corresponding percentages in infected cells ($n=5$) were $14.2\pm1.1$, $2.7\pm1.1$ and $3.5\pm1.4\%$, respectively, and they were not significantly different from the counterparts. On the basis of these findings, such crude $I_{Na}$ was used for evaluation of the effect of the viral infection on $I_{Na}$. Hereafter, the crude $I_{Na}$ was designed as $I_{Na}$.

The values in the text are expressed as means±s.e.mean with the number of cells ($n$) used for measurements. Statistical significance was tested using a Student's unpaired $t$-test and differences were considered significant when $P<0.05$.

### *Solutions*

PSS used in the experiments had the following composition (mM); NaCl 120, KCl 5, $CaCl_2$ 1.8, $MgCl_2$ 1, glucose 25, 2-[4-(2-hydroxyethl)-1-piperazinyl]ethanesulphonic acid (HEPES) 5 (titrated to pH 7.4 with NaOH). The KCl was replaced with equimolar CsCl when $I_{Na}$ was measured. In some experiments dealing with $I_{K\text{-}IR}$, KCl in PSS was increased to 40 mM by replacing equimolar NaCl with it.

Two kinds of pipette solution were used. One, a $K^+$-based solution, had the following composition (mM); KOH 120, KCl 5, L-glutamic acid 115, NaCl 10, $MgCl_2$ 2.5, glucose 5, piperazine-N,N′-bis(2-ethanesulphonic acid) 5, EGTA 5, (titrated to pH 7.0 with KOH). The other, a $Cs^+$-based solution, had the composition that $K^+$ in the $K^+$-based solution was replaced with $Cs^+$.

### *Drugs and medium*

Tetrodotoxin (TTX), tetraethylammonium chloride (TEA) and nifedipine were purchased from Wako (Osaka City, Osaka, Japan). Eagle's minimum essential medium was from Nissui (Toshima-ku, Tokyo, Japan).

## Results

### *Microscopic observation*

Rabies virus-infected cells prepared on a coverslip were bathed in PSS and examined under a light-microscopy (×400). Most

of the cells (*c.a.* 80%) had a round cell body of 20–30 $\mu$m in diameter and one or more neurites of 5–100 $\mu$m in length. The remaining cells had no visual neurite and a greater variation in cell size. There was no appreciable difference in morphological profile between infected and uninfected cells. However, the cytoplasm of many infected cells seemed somewhat mottled, perhaps because of multivesicular vacuolization (Iwasaki & Clark, 1977).

Regardless of virus infection, cells with a round shape of 20–30 $\mu$m in diameter and 50 $\mu$m or shorter neurites, which are separated from any neighbouring cells, were chosen for the following patch clamp investigation.

### *Depolarization-induced membrane currents*

To characterize current activated by membrane depolarization, uninfected cells, bathed in PSS, dialyzed with $K^+$-based pipette solution and held at a holding potential of $-80$ mV, were stepped by application of a 200 ms depolarizing pulse to 10–20 mV. The membrane depolarization elicited a biphasic current; a transient inward current followed by a sustained outward current lasting the pulse duration. The transient inward component of the current was due to activation of voltage-gated $Na^+$ channels, since it was abolished after application of 1 $\mu$M TTX, a $Na^+$ channel blocker, but it remained unaltered after application of $Ca^{2+}$ channel blockers such as 5 $\mu$M nifedipine, 100 $\mu$M $Ni^{2+}$ and 100 $\mu$M $Cd^{2+}$. The outward component of the current was characterized by a slow activation and little or no inactivation over the period of 100–200 ms, and blocked after application of 20 mM TEA, a $K^+$ channel blocker. These characteristics of the outward current were similar to those described for a delayed rectifier $K^+$ current ($I_{K\text{-}DR}$) (Rudy, 1988).

No evidence for activation of voltage-gated $Ca^{2+}$ channels was obtained even when $Cs^+$-based pipette solution was used to block $K^+$ currents including $I_{K\text{-}DR}$ which counteract inward $Ca^{2+}$ current, or when $Ba^{2+}$ (up to 60 mM), a more permeable cation to the $Ca^{2+}$ channels than $Ca^{2+}$, was used as a charge carrier ($n=5$).

These results showed that in uninfected NA cells, two types of depolarization-evoked current, namely $I_{Na}$ and $I_{K\text{-}DR}$, could be detected.

### *Effect of rabies virus infection on $I_{Na}$ and $I_{K\text{-}DR}$*

$I_{Na}$ was recorded alternately from infected and uninfected cells under such conditions as $K^+$ current was blocked by means of dialysis with $Cs^+$-based pipette solution. No compensation of series resistance was made because the whole-cell patch clamp configuration could not be maintained with a high seal resistance when the compensation circuitry was used. Cells were held at $-80$ mV and stepped every 10 s with 50 ms pulses to varied potentials ranging from $-70$ to 50 mV in 10 mV increments. Figure 1A shows representative traces of $I_{Na}$ recorded from an uninfected cell and an infected cell. $I_{Na}$ was elicited upon stepping to potentials between $-30$ and 40 mV, and its maximum amplitude was attained at a potential of $-10$ mV. Figure 1B shows the averaged current-voltage relationships obtained from $I_{Na}$ recordings from 20 uninfected cells and 22 infected cells. It can be seen that the mean peak amplitude of $I_{Na}$ at every potential was smaller in infected cells than uninfected cells, with a significant difference ($P<0.05$) over the potential range of $-20$ to 20 mV. The mean peak amplitude of $1071\pm68$ pA ($n=20$) was reduced to $625\pm72$ pA ($n=22$) following the viral infection. However, the time taken for the $I_{Na}$ to reach its peak and the time taken to decay from its peak to half peak amplitude of $4.3\pm0.5$ ms and $1.6\pm0.1$ ms ($n=22$) in infected cells, respectively, were not significantly different from the corresponding values in uninfected cells ($4.0\pm0.3$ ms and $1.3\pm0.2$ ms, $n=20$, respectively).

The current-voltage relationships in the both groups of cell are shown in Figure 1B. The ascending limb of the curve seemed to become less steep over the voltage between $-40$ and 0 mV after the viral infection. To examine this, the voltage-

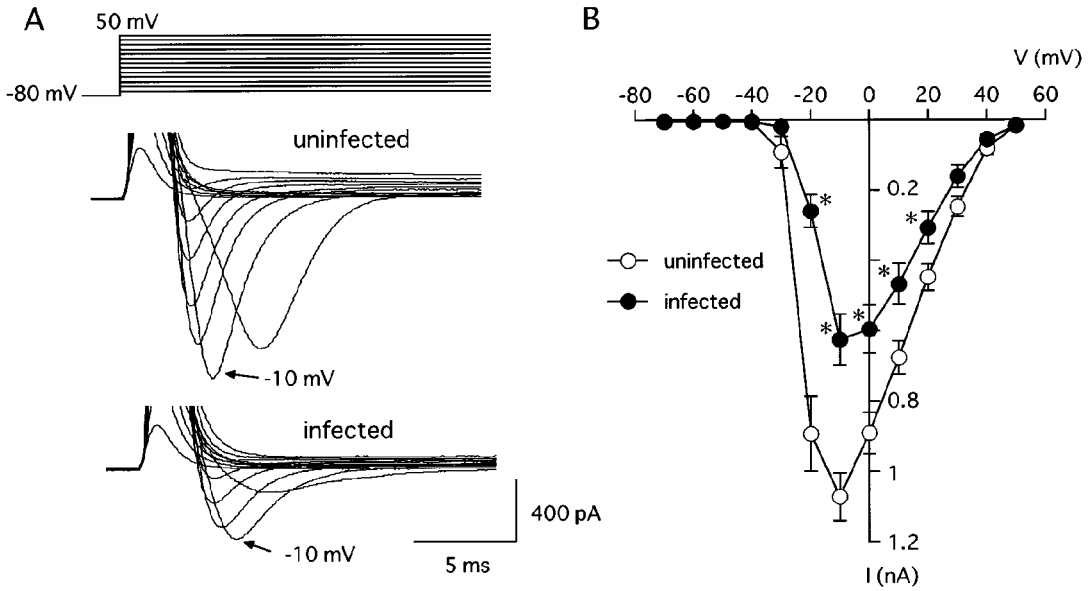


**Figure 1** Voltage-dependent $Na^+$ current ($I_{Na}$) in uninfected and infected NA cells. The cells were held at $-80$ mV using a patch pipette filled with $Cs^+$-based pipette solution to block $K^+$ current. To activate $I_{Na}$, 50 ms step pulses to various potentials ranging from $-70$ to 50 mV in 10 mV increments were applied every 10 s (see top traces in A). (A) Superimposed recording traces of $I_{Na}$ evoked by the sequential step pulses in an uninfected cell (middle trace) and an infected cell (bottom trace). (B) Averaged current-voltage relationships of peak $I_{Na}$ from 20 uninfected and 22 infected cells. Each point indicates the mean$\pm$s.e.mean (vertical lines). *, Significant difference ($P<0.05$) from the corresponding value for the uninfected cell.

dependence of $I_{Na}$ activation was quantified using data obtained from the experiments in Figure 1. $Na^+$ conductance of the membrane ($G_{Na}$) activated by step pulses to potentials of up to 0 mV was calculated by dividing $I_{Na}$ amplitude by the driving force for $Na^+$, namely a potential difference between $Na^+$ equilibrium potential ($E_{Na} = 64.8$ mV) and membrane potential achieved by the step pulses. $G_{Na}$ was plotted against the membrane potential by fitting the data by a least square method with the Boltzmann function, $G_{Na} = G_{Na\text{-}max}/\{1+\exp[(V_{0.5}-E_m)/\kappa]\}$, where $G_{Na\text{-}max}$ is the maximal $G_{Na}$, $V_{0.5}$ is the potential of half-maximal activation of $G_{Na}$, $E_m$ is membrane potential and $\kappa$ is slope factor. Figure 2 shows averaged activation curves of $G_{Na}$ obtained from 22 infected cells and 20 uninfected cells. It can be seen that the viral infection shifts the activation curve by some 6 mV in the positive direction along the voltage axis with decreased slope and $G_{Na\text{-}max}$. In the infected cells, the mean values for $G_{Na\text{-}max}$, $V_{0.5}$ and $\kappa$ were $9.2 \pm 1.1$ nS, $-17.3 \pm 0.9$ mV and $3.2 \pm 0.1$ ($n = 22$), respectively, each of which was significantly different ($P < 0.05$) from the corresponding value for the uninfected cells ($G_{Na\text{-}max}$, $14.0 \pm 0.9$ nS; $V_{0.5}$, $-23.1 \pm 0.9$ mV; $\kappa$, $2.0 \pm 0.2$, $n = 20$).

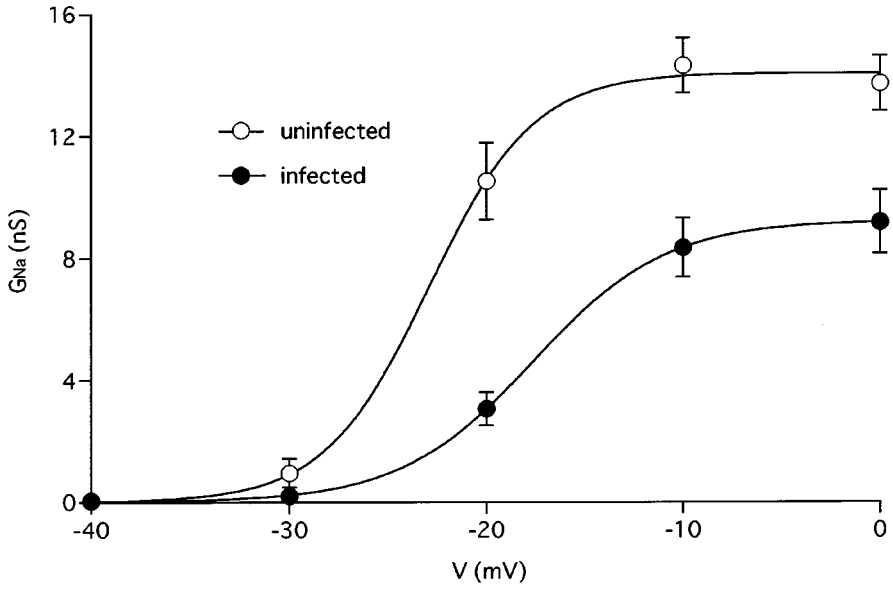


**Figure 2** Averaged $Na^+$ conductance ($G_{Na}$)-voltage relationships in infected and uninfected NA cells. Each point indicates the mean $\pm$ s.e.mean (vertical lines) of measurements in 20 uninfected cells or 22 infected cells. The points were fitted by the Boltzmann function. See text for details.

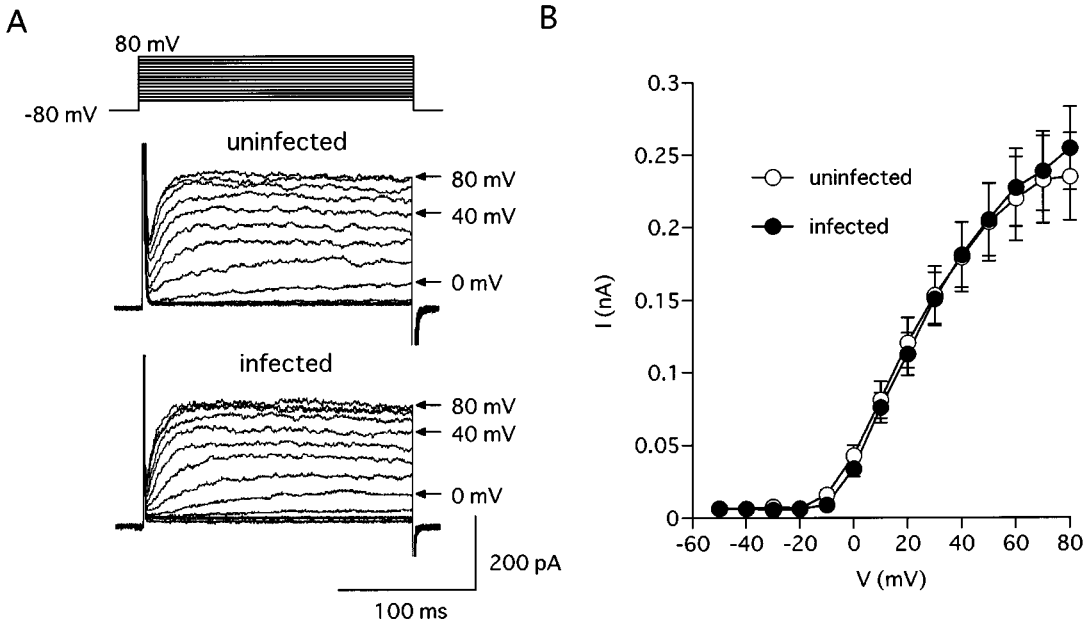


**Figure 3** Delayed rectifier $K^+$ current ($I_{K\text{-}DR}$) in uninfected and infected NA cells. The cells were bathed in 1 $\mu$M TTX-containing PSS and held at $-80$ mV using a patch pipette filled with $K^+$-based pipette solution. To activate $I_{K\text{-}DR}$, 200 ms step pulses, to potentials ranging from $-50$ to 80 mV in 10 mV increments, were applied every 10 s (see top traces in A). (A) Superimposed recording traces of $I_{K\text{-}DR}$ evoked by the sequential step pulses in an uninfected cell (middle trace) and in an infected cell (bottom trace). (B) Averaged current-voltage relationships of peak $I_{K\text{-}DR}$ from 14 uninfected and 16 infected cells. Each point indicates the mean $\pm$ s.e.mean (vertical lines).

$I_{K\text{-}DR}$ was recorded from infected and uninfected cells, bathed in TTX (1 $\mu$M)-containing PSS to block $I_{Na}$ and dialysed with $K^+$-based pipette solution. Step pulses (200 ms in duration) to $-50$ mV or more positive potentials (up to 80 mV) from the holding potential of $-80$ mV were used to evoke $I_{K\text{-}DR}$. The pulses were applied in 10 mV increments every 10 s. In all of 16 infected cells as well as 14 uninfected cells, $I_{K\text{-}DR}$ was activated at potentials more positive than $-10$ mV (Figure 3A). The peak amplitude of $I_{K\text{-}DR}$ increased in a voltage-dependent manner. As shown in Figure 3B, the averaged current-voltage relationships for the infected and the uninfected cells almost overlapped. There was no noticeable difference in the shape of current responses between the two groups of cells (see Figure 3A).

Before starting recording of $I_{Na}$ or $I_{K\text{-}DR}$, membrane capacitance was measured by applying a 10 mV hyperpolarizing pulse. The mean membrane capacitance was $28.9 \pm 2.2$ pF ($n=38$) for the infected cell and $31.8 \pm 1.8$ pF ($n=34$) for the uninfected cell. There was no significant difference between the mean values.

The results suggest that rabies virus infection causes a reduced functional expression of voltage-dependent $Na^+$ channels but not delayed rectifier $K^+$ channels.

### *Effect of rabies virus infection on the resting membrane potential and membrane resistance*

Cells were bathed in PSS and dialysed with $K^+$-based pipette solution, and the resting membrane potential was measured under current clamp mode some 5 min after achievement of the whole-cell patch clamp configuration. In infected cells, the mean resting membrane potential was $-18.7 \pm 2.2$ mV ($n=19$), which was significantly different ($P<0.01$) from the corresponding value in uninfected cells ($-33.1 \pm 2.2$ mV, $n=18$) (see Figure 4A). The resting membrane potentials were comparable with those reported for other neuroblastoma cell types ($-48$ to $-20$ mV, Arcangeli *et al*., 1995; $-39 \pm 2$ mV, Higashida *et al*., 1983).

To evoke electrotonic potentials, hyperpolarizing current pulses (1 s in duration) were applied at varied intensities from 5–30 pA in 5 pA increments every 10 s. In either infected or uninfected cells, the size of electrotonic potentials increased depending on the current intensity (Figure 4A). Figure 4B shows plots of the size of the electrotonic potentials against the current intensity. Data points in the graph represent mean values of measurements in 19 infected cells and in 18 uninfected cells. The relationship between the two variables was linear from zero up to 15 pA, giving regression lines expressed by $y=3.15\ x-18.9$ ($r=0.99$; $P<0.05$) for the infected cell and by $y=2.20\ x-34.1$ ($r=1.00$; $P<0.05$) for the uninfected cell, where y is membrane potential and x is the current intensity. The steeper slope of the regression line in the infected cell suggested a higher membrane input resistance. The mean membrane input resistance, estimated from electrotonic potentials evoked by 15 pA current pulse, was $3.13 \pm 0.31$ G$\Omega$ ($n=19$), which was significantly greater ($P<0.05$) than the corresponding value for the uninfected cell ($2.23 \pm 0.26$ G$\Omega$, $n=18$). The mean membrane time constant was also estimated to be $0.20 \pm 0.02$ s ($n=19$), which was significantly longer ($P<0.05$) than the uninfected cell ($0.14 \pm 0.01$ s, $n=18$). Two regression lines crossed each other at a membrane potential of $-69.3$ mV. The membrane potential was close to the equilibrium potential for $K^+$ ($-82.1$ mV) estimated from the $K^+$ gradient across the cell membrane.

These results indicate that rabies virus infection causes a decrease in the activity of some type of $K^+$ channels in the membrane, resulting in a decrease in the resting membrane potential (depolarization) and an increase in the membrane input resistance.

As in neuroblastoma cells, inward rectifier $K^+$ channels have been suggested to play a role in determining the resting membrane potential (Arcangeli *et al*., 1995), effect of rabies virus infection on this type of $K^+$ channel was tested.

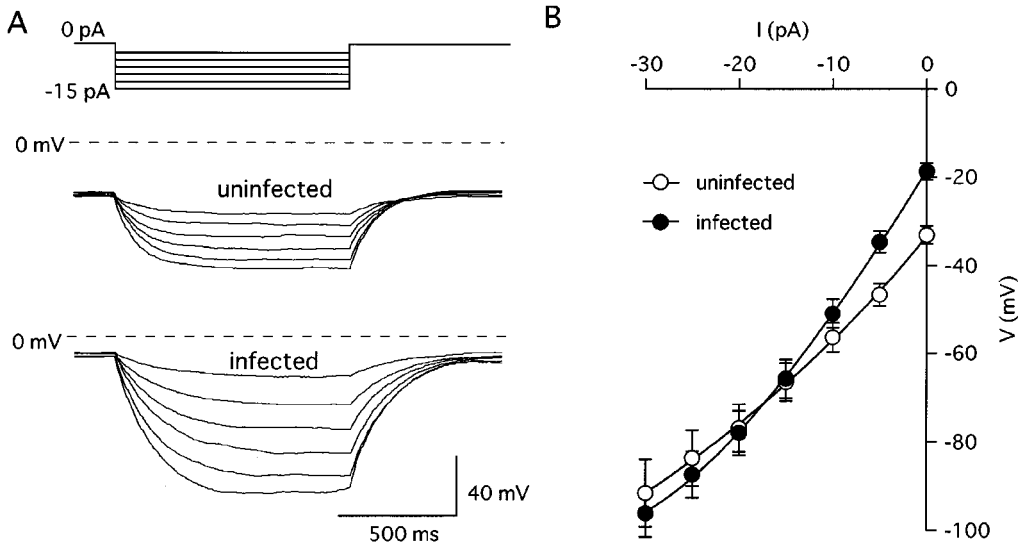


**Figure 4** Changes in membrane potential (electrotonic potentials) elicited by hyperpolarizing current pulses in uninfected and infected NA cells. The cells were dialyzed with $K^+$-based pipette solution and held under current clamp mode. The current pulses (1 s in duration) of intensities varied from 5–30 pA in 5 pA increments were applied every 10 s (see top traces in A). (A) Superimposed recording traces of electrotonic potentials elicited by the sequential current pulse applications in an uninfected cell (middle trace) and in an infected cell (bottom trace). Interrupted lines indicate the zero mV level. (B) Plots of membrane potential attained by electrotonic potentials against the current intensity in uninfected and infected cells. Each point represents the mean $\pm$ s.e.mean of measurements in 18 uninfected or 19 infected cells. The solid lines were drawn by eyes. See text for details.

*Effect of rabies virus infection on membrane current flowing through inward rectifier $K^+$ channels ($I_{K\text{-}IR}$)*

Current recordings were made from cells bathed in a 40 mM $K^+$-containing PSS and dialyzed with $K^+$-based pipette solution. The ionic conditions gave a reversal potential for $K^+$ of $-28.4$ mV. The cells were held at 0 mV, and when 200 ms hyperpolarizing pulses to various potentials ranging from $-40$ up to $-140$ mV in 10 mV increments were applied every 10 s, an inward current lasting the pulse duration was elicited, as shown in Figure 5A. The inward current was reversibly blocked after extracellular application of 20 mM $Cs^+$ or $Ba^{2+}$, as described for $I_{K\text{-}IR}$ in other cells (Stelling & Jacob, 1992, Gay & Stanfield, 1977). Thus, the inward current was considered to be $I_{K\text{-}IR}$.

$I_{K\text{-}IR}$ evoked in infected cells was similar in the time course to that evoked in uninfected cells. As shown in Figure 5A, the rates at which $I_{K\text{-}IR}$ reached its peak and then declined to a sustained level increased as the pulse potential was increased in the negative direction. For $I_{K\text{-}IR}$ activated at $-140$ mV in infected cells, the time to peak and half decay time were $8.6\pm0.4$ ms and $15.9\pm1.5$ ms ($n=17$), respectively. The mean values did not significantly differ from the corresponding values obtained from uninfected cells ($9.4\pm0.4$ ms for time to peak and $18.5\pm1.5$ ms for half decay time, $n=22$).

Figure 5B shows roughly linear current-voltage relationships of $I_{K\text{-}IR}$ in the absence and presence of rabies virus infection. It is clear that the mean peak amplitude of $I_{K\text{-}IR}$ was significantly smaller ($P<0.01$) at any potential in infected cells (for example, at $-80$ mV, $71\pm12$ pA ($n=23$) in infected cells and $162\pm20$ pA ($n=22$) in uninfected cells). Furthermore, it can be seen that the mean peak amplitude was reduced to 42–47% after rabies virus infection at any potentials.

The results suggest that the functional expression of inward rectifier $K^+$ channels is decreased after rabies virus infection.

## Discussion

In the present study, we investigated effect of rabies virus infection on three types of membrane current detected in mouse neuroblastoma NA cells, namely voltage-dependent $Na^+$ current ($I_{Na}$), delayed rectifier $K^+$ current ($I_{K\text{-}DR}$) and inward rectifier $K^+$ current ($I_{K\text{-}IR}$). The results suggest that the viral infection reduces the functional expression of voltage-dependent $Na^+$ channels and inward rectifier $K^+$ channels without changing that of delayed rectifier $K^+$ channels.

Any detectable difference in cell morphology was not observed in infected cells by the microscopic examination. This was supported by the fact that measurements of membrane capacitance did not give any significant difference between infected cells and uninfected cells. It is known that rabies viruses begin to bud off from host cells within 1 day postinfection (personal communication; Minamoto). This suggests that at the stage of the viral infection when rabies viruses begin to bud off from host cells, some invisible structural changes in the plasma membrane may occur, which lead to nonselective dysfunction of different types of ion channel. However, the result that unlike $I_{Na}$ and $I_{K\text{-}IR}$, $I_{K\text{-}DR}$ remained unchanged after infection with the virus for 3 days does not support the idea that the viral infection results in nonselective dysfunction of different types of ion channel. The selective reduction of $I_{Na}$ and $I_{K\text{-}IR}$ can be more easily explained by assuming interaction of penetrated rabies virions and/or synthesized rabies structural proteins with some intracellular factor(s).

There are only some pieces of circumstantial evidence so far; oligonucleosomal DNA fragmentation occurs during

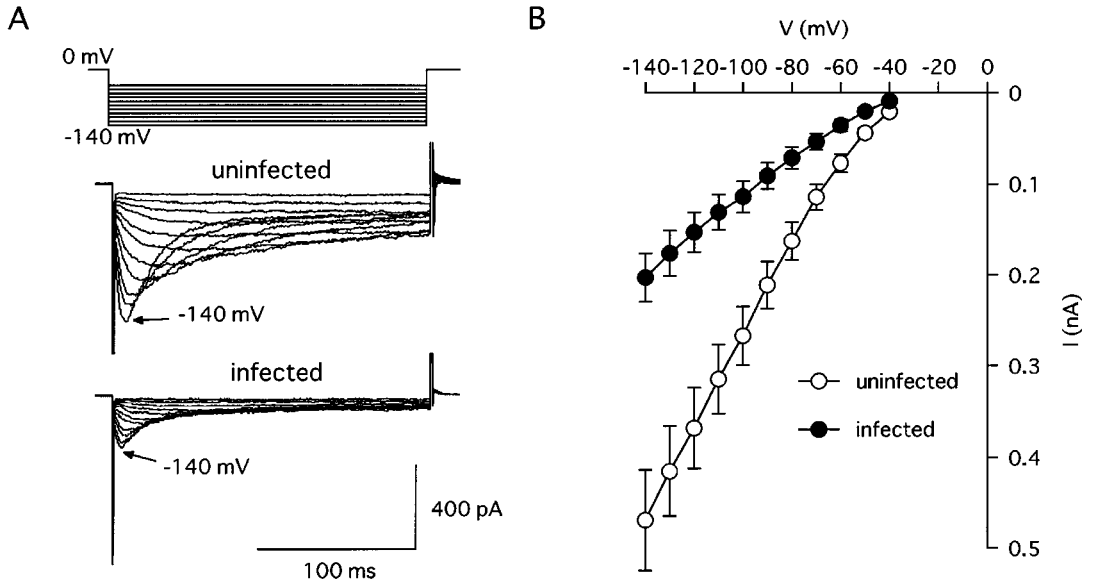


**Figure 5** Inward rectifier $K^+$ current ($I_{K\text{-}IR}$) in uninfected and infected NA cells. The cells were bathed in a 40 mM $K^+$-containing PSS and held at 0 mV using a pipette filled with $K^+$-based pipette solution. To activate $I_{K\text{-}IR}$, 200 ms step pulses to various potentials ranging from $-40$ to $-140$ mV in 10 mV increments were applied every 10 s (see top traces in A). (A) Superimposed recording traces of $I_{K\text{-}IR}$ evoked by the sequential voltage steps in an uninfected cell (middle trace) and in an infected cell (bottom trace). (B) Averaged current-voltage relationships of peak $I_{K\text{-}IR}$ from 22 uninfected and 23 infected cells. Each point indicates the mean$\pm$s.e.mean (vertical lines). At any potential between $-40$ and $-140$ mV, the mean value for the infected cell differed significantly ($P<0.01$) from the corresponding value for the uninfected cell.

rabies virus infection (Jackson & Rossiter, 1997; Jackson & Park, 1998), and synthesis of nucleic acids and proteins is inhibited after infection with vesicular stomatitis virus that belongs to the same family, rhabdoviridae, as rabies virus (Marcovistz *et al*., 1983; Francouer & Stanners, 1978). Further study needs to elucidate mechanisms underlying the reduction of functional expression of channels carrying $I_{Na}$ and $I_{K\text{-}IR}$ in rabies virus-infected NA cells.

In rat cortical cultured neurons, rabies virus infection causes a reduction of GABA uptake, and the effect is considered to occur as a result of membrane depolarization in virus-infected neurons (Ladogana *et al*., 1994). The present finding that infected NA cells had the decreased resting membrane potential is favourable for such idea. The membrane depolarization in infected NA cells was associated with a reduction of $I_{K\text{-}IR}$. As in other several cell types (Arcangeli *et al*., 1995), inward rectifier $K^+$ channels seem likely to be involved in determination of the resting membrane potential.

There are many studies suggesting that functional impairment of neurotransmitter receptors such as muscarinic ACh receptors, opiate receptors and serotonin receptors, is involved in the pathogenesis of rabies disease (Tsiang, 1993). To our knowledge, the present study first showed that rabies virus infection alters functional expression of ion channels in host cells. It is well established that the voltage-dependent $Na^+$ channels are activated during the upstroke of action potentials in excitable cells including neurons. In the central nervous system, which is the predilection site for rabies virus infection, an action potential serves for neuro-neuronal transmission by triggering release of the neurotransmitter. The observation of $I_{Na}$ reduction obtained from infected NA cells leads us to suppose that rabies virus infection may prevent host neurons in the central nervous system from firing action potentials and as a result, neuro-neuronal transmission is interfered. The $I_{K\text{-}IR}$ reduction leading to membrane depolarization suggests that the membrane depolarization of host neurons which takes place following the virus infection affects the generation of synaptic potentials and action potentials. In these respects, the present results provide evidence for involvement of an alteration in the membrane properties associated with reduced functional expression of the ion channels in the pathogenesis of rabies disease.

This work was supported by a Grant-in-Aid for Scientific Research (08456150) from Ministry of Education, Science and Culture, Japan.

## References


ARCANGELI, A., BIANCHI, L., BECCHETTI, A., FARAVELLI, L., CORONNELLO, M., MINI, E., OLIVOTTO, M. & WANKE, E. (1995). A novel inward-rectifying $K^+$ current with a cell-cycle dependence governs the resting potential of mammalian neuroblastoma cells. *J. Physiol.,* **489,** 455–471.

BAKHRAMOV, A., BORISKIN, Y.S., BOOTH, J.C. & BOLTON, T.B. (1995). Activation and deactivation of membrane currents in human fibroblasts following infection with human cytomegalovirus. *Biochimica et Biophysica Acta,* **1265,** 143–151.

BAUMGOLD, J. & SPECTOR, I. (1987). Development of sodium channel protein during chemically induced differentiation of neuroblastoma cells. *J. Neurochem.,* **48,** 1264–1269.

CECCALDI, P.E., FILLION, M.P., ERMINE, A., TSIANG, H. & FILLION, G. (1993). Rabies virus selectively alters 5-$HT_1$ receptor subtypes in rat brain. *Eur. J. Pharmacol.,* **245,** 129–138.

CLEJAN, S., DOTSON, R.S., WOLF, E.W., CORB, M.P. & IDE, C.F. (1996). Morphological differentiation of N1E-115 neuroblastoma cells by dimethyl sulfoxide activation of lipid second messengers. *Exp. Cell Res.,* **224,** 16–27.

DUMRONGPHOL, H., SRIKIATKHACHORN, A., HEMACHUDH, T., KOTCHABHAKDI, N. & GOVITRAPONG, P. (1996). Alteration of muscarinic acetylcholine receptors in rabies viral-infected dog brains. *J. Neurolog. Sci.,* **137,** 1–6.

FRANCOUER, A.M. & STANNERS, C.P. (1978). Evidence against the role of $K^+$ in the shut-off of protein synthesis by vesicular stomatitis virus. *J. Gen. Virol.,* **39,** 551–553.

GAY, L.A. & STANFIELD, P.R. (1977). $Cs^+$ causes a voltage-dependent block of inward K currents in resting skeletal muscle fibres. *Nature,* **267,** 169–170.

HAMILL, O.P., MARTY, A., NEHER, E., SAKMANN, B. & SIGWORTH, F.J. (1981). Improved patch-clamp techniques for high-resolution current recording from cells and cell-free membrane patches. *Pflugers Archiv - Eur. J. Physiol.,* **391,** 85–100.

HIGASHIDA, H., SUGIMOTO, N., OZUTSUMI, K., MIKI, N. & MATSUDA, M. (1983). Tetanus toxin: a rapid and selective blockade of the calcium, but not sodium, component of action potentials in cultured neuroblastoma N1E-115 cells. *Brain Res.,* **279,** 363–368.

ITO, H., MINAMOTO, N., WATANABE, T., GOTO, H., RONG, L.T., SUGIYAMA, M., KINJO, T., MANNEN, K., MIFUNE, K., KONOBE, T, YOSHIDA, T. & TAKAMIZAWA, A. (1994). A unique mutation of glycoprotein gene of the attenuated RC-HL strain of rabies virus, a seed virus used for production of animal vaccine in Japan. *Microbiol. Immunol.,* **38,** 479–482.

IWASAKI, Y. & CLARK, H.F. (1977). Rabies virus infection in mouse neuroblastoma cells. *Lab. Investigat.,* **36,** 578–584.

JACKSON, A.C. & PARK, H. (1998). Apoptotic cell death in experimental rabies in suckling mice. *Acta Neuropathol.,* **95,** 159–164.

JACKSON, A.C. & REIMER, D.L. (1989). Pathogenesis of experimental rabies in mice: an immunohistochemical study. *Acta Neuropathol.,* **78,** 159–165.

JACKSON, A.C. & ROSSITER, J.P. (1997). Apoptosis plays an important role in experimental rabies virus infection. *J. Virol.,* **71,** 5603–5607.

JOHNSON, R.T. (1965). Experimental rabies. Studies of cellular vulnerability and pathogenesis using fluorescent antibody staining. *J. Neuropathol. Exp. Neurol.,* **24,** 662–674.

LADOGANA, A., BOUZAMONDO, E., POCCHIARI, M. & TSIANG, H. (1994). Modification of tritiated $\gamma$-amino-n-butyric acid transport in rabies virus-infected primary cortical cultures. *J. Gen. Virol.,* **75,** 623–627.

MARCOVISTZ, R., ERMINE, A. & TSIANG, H. (1983). Protein synthesis in VSV infected CNS, neuroblastoma and BHK cell lines. *Microbiol.,* **6,** 293–304.

MCMORRIS, F.A. & RUDDLE, F.H. (1974). Expression of neuronal phenotypes in neuroblastoma cell hybrids. *Dev. Biol.,* **39,** 226–246.

MINAMOTO, N., TANAKA, H., HISHIDA, M., GOTO, H., ITO, H., NARUSE, S., YAMAMOTO, K., SUGIYAMA, M., KINJO, T., MANNEN, K. & MIFUNE, K. (1994). Linear and conformation-dependent antigenic sites on the nucleoprotein of rabies virus. *Microbiol. Immunol.,* **38,** 449–455.

MUNZEL, P. & KOSCHEL, K. (1981). Rabies virus decreases agonist binding to opiate receptors of mouse neuroblastoma-rat glioma hybrid cells 108-cc-15. *Biochem. Biophys. Res. Commun.,* **101,** 1241–1250.

RUDY, B. (1988). Diversity and ubiquity of K channels. *Neurosci.,* **25,** 729–749.

SMART, N.L. & CHARLTON, K.M. (1992). The distribution of Challenge virus standard rabies virus versus skunk street rabies virus in the brains of experimentally infected rabid skunks. *Acta Neuropathol.,* **84,** 501–508.

STELLING, J.W. & JACOB, T.J. (1992). The inward rectifier $K^+$ current underlies oscillatory membrane potential behaviour in bovine pigmented ciliary epithelial cells. *J. Physiol.,* **458,** 439–456.

SUGAMATA, M., MIYAZAWA, M., MORI, S., SPANGRUDE, G.J., EWALT, L.C. & LODMELL, D.L. (1992). Paralysis of street rabies virus-infected mice is dependent on T lymphocytes. *J. Virol.,* **66,** 1252–1260.

TIRAWATNPONG, S., HEMACHUDHA, T., MANUTSATHIT, S., SHUANGSHOTI, S., PHANTHUMCHINDA, K. & PHANUPHAK, P. (1989). Regional distribution of rabies viral antigen in central nervous system of human encephalitic and paralytic rabies. *J. Neurol. Sci.,* **92,** 91–99.

TSIANG, H. (1982). Neuronal function impairment in rabies-infected rat brain. *J. Gen. Virol.,* **61,** 277–281.

TSIANG, H. (1993). Pathophysiology of rabies virus infection of the nervous system. *Adv. Virus Res.,* **42,** 375–412.

*(Received September 23, 1998*
*Accepted January 19, 1999)*